# Study on copper precipitation during continuous heating and cooling of HSLA steels using electrical resistivity

**A. N. Bhagat*[1], S. K. Pabi[2], S. Ranganathan[3] and O. N. Mohanty[4]**

Electrical resistivity technique was used to study the phase transformation and copper precipitation during continuous heating and cooling of three Cu bearing high strength low alloy (HSLA) steels. Dilatation measurements were performed to compare the results with the resistivity. During heating, the dilatation plot revealed $Ac_1$ and $Ac_3$ temperature, while resistivity measurements indicated precipitation of copper in the range of 370–550°C. A method was demonstrated to estimate the amount of copper precipitation during continuous heating. During continuous cooling, the austenite transformation temperatures could be derived from resistivity, which compare well with dilatometry. A hysteresis between heating and cooling curve was noted possibly owing to formation of bainite during cooling. Non-isothermal kinetic analysis of dilatation data during continuous cooling yields an activation energy of 62 kJ $mol^{-1}$, which could be related to the formation of bainite, whereas higher activation energy of 237 kJ $mol^{-1}$ obtained from resistivity data may correspond to the diffusion of Cu in iron, associated with the copper precipitation during austenite transformation.

**Keywords:** HSLA steel, Continuous cooling transformation, Copper precipitation, Electrical resistivity, Activation energy



## Introduction

Copper containing high strength low alloy (HSLA) steels, like HSLA-80 and HSLA-100 possess a combination of strength, toughness and corrosion properties often demanded for naval structural applications typically in large submarines, offshore structures, line pipes and hull of ships, etc.[1,2] Copper is the prime alloying element in these steels, which provides strength by classical age hardening in addition to improvement in the corrosion resistance. The precipitation of copper in iron base systems during aging has been studied by several investigators,[3–10] however only a few reports[11–13] are available on the precipitation of copper in HSLA steels, i.e. in a multi alloying environment. Various techniques, such as TEM, field ion microscopy (FIM), small angle neutron scattering (SANS) and so on, have been used to assess the size, shape and distribution of the copper precipitates[3–13] but these tools are inadequate to estimate the amount of fine coherent copper precipitates occurring during initial stage of aging. It is reported that during aging, copper initially appears as coherent nanometre size (<5 nm) spherical precipitates.[3–9] These precipitates are difficult to detect by conventional TEM[8–10] and can be revealed by other techniques such as SANS and FIM. For longer aging time, these coherent precipitates transform to incoherent particles, which can be easily detected by TEM.[6,9,12–16] Dilatation technique is well known for phase transformation studies from austenite to ferrite and vice versa but it is insensitive to study precipitation of copper in steel. Measurement of electrical resistivity continuously as a function of temperature is an effective means of studying the precipitation in steel. This tool has been used for a few elements in steels[17–20] but none has used to study the precipitation of copper in HSLA steels in complex alloying environment.

Electrical resistivity data for one HSLA steel have been reported elsewhere;[21] in the present communication, the results of studies on three HSLA steels with varying amounts of copper content have been presented. A major focus of the present work is to show that the precipitation of coherent fine particles of copper during heating, which cannot be detected by TEM, can be estimated using electrical resistivity. In addition, kinetics of phase transformation during continuous cooling has also been assessed using resistivity and dilatation data.

## Experimental

Three varieties of HSLA steels (S1, S2 and S3) and one low carbon steel (LCS) were used in this study. The chemical compositions of the steels analysed by optical emission spectroscopy method are reported in Table 1.

[1]Tata Steel, Jamshedpur, Jharkhand, Pin 831007, India
[2]Department of Metallurgical and Materials Engineering, IIT Kharagpur, WB, Pin-721302, India
[3]National Metallurgical Laboratory, Jamshedpur, Jharkhand, Pin-831007, India
[4]Biju Patnayak University of Technology, Bhubneshwar, Pin-751003, India

*Corresponding author, email anbhagat@tatasteel.com


Published by Maney on behalf of the Institute
Received 31 March 2006; accepted 19 June 2006
DOI 10.1179/174328407X157218

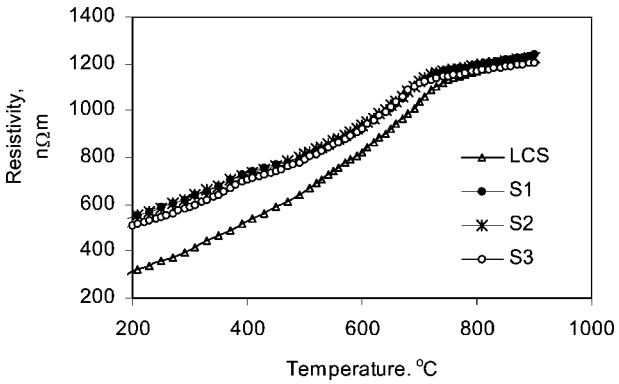


**1 Electrical resistivity as function of temperature during continuous heating (0·33 K $s^{-1}$) for low carbon steel and HSLA steels**

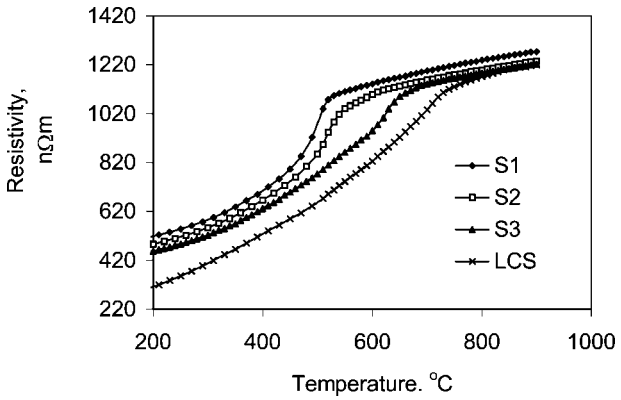


**2 Electrical resistivity as function of temperature during continuous cooling (0·33 K $s^{-1}$) for low carbon steel and HSLA steels**

The HSLA steels were obtained in plate form in the thickness range of 32–50 mm from the Naval Research laboratory, Washington DC, USA. The LCS was obtained from 25 mm thick transfer bar of Hot Strip Mill of Tata Steel Company.

Resistivity studies were conducted on the HSLA and LCS. As received samples were machined to 8 mm diameter rods. These rods were then drawn to 0·5 mm diameter wires in successive passes with intermediate annealing at 900°C. These wires were annealed at 900°C in vacuum ($10^{-6}$ Torr) for 1 h and then cooled in the furnace. The annealed wires of ~100 mm length were placed in quartz capsules, which were repeatedly flushed with argon and evacuated. The sealed capsules were heated to 900°C, held at that temperature for 1 h and quenched in water. The quenched wire sample of ~20 mm length was welded to the sample holder of the resistivity apparatus (Sinko-Riko). The samples of both steels were heated in vacuum to 900°C at a rate of 0·33 K $s^{-1}$ and cooled at the same rate in the evacuated chamber of the resistivity apparatus. The potential drop across the wire was continuously recorded as a function of temperature. The resistivity $\rho$ and the gradient $d\rho/dT$ were calculated and plotted as a function of temperature. Dilatometric studies were conducted using 6 mm diameter cylindrical specimens on thermomechanical simulator Gleeble-1500 for S1 and S2 steels. Dilatation as a function of temperature was recorded during continuous heating and cooling at a rate of 0·33 K $s^{-1}$.

# Results

## Resistivity measurements

The resistivity data for all three HSLA steels and LCS were continuously recorded as a function of temperature during heating and cooling. The $\rho$–$T$ plot during continuous heating for these steel has been presented in Fig. 1, which shows a continuous rise with increasing temperature. It also shows that the resistivity curves for all HSLA steels are similar and located higher than those for LCS in the temperature range of 100–770°C. It is known that the resistivity of a metal increases with increasing temperature, but the difference in resistivity between HSLA and LCS may be attributed to the alloying effect, such as Mn, Cr, Si, Ni and Cu present in the HSLA steels (Table 1). These elements are reported to increase the resistivity.[22,23] It is also apparent from Fig. 1 that the difference in $\rho$ between HSLA and LCS decreases with increasing temperature and beyond 770°C the data practically merge for all steels. The resistivity of pure iron and a number of alloy steels have shown a similar converging trend in austenite.[24] It is apparent that the effect of alloying elements on the resistivity in the paramagnetic phase (above ~770°C, the Curie temperature of iron) is not significant. During continuous cooling, $\rho$ versus $T$ plots for HSLA and LCS have been presented in Fig. 2. In this case, the resistivity follows the straight line behaviour up to a lower temperature for HSLA steels. The difference in resistivity behaviour between LCS and HSLA steels may be attributed to the difference in the transformation characteristics. During heating, initial 'bcc/bct' structure transforms to austenite while during cooling, transformation product in the case of HSLA steel may be different.

**Table 1 Chemical compositions of HSLA and low carbon steels (wt-%)**

| Steel | C | Mo | Cr | Mn | Cu | Ni | Nb | Al | N | Si |
|---|---|---|---|---|---|---|---|---|---|---|
| S1 | 0·038 | 0·57 | 0·54 | 0·87 | 1·98 | 3·39 | 0·032 | 0·038 | 0·0145 | 0·23 |
| S2 | 0·04 | 0·60 | 0·57 | 0·86 | 1·58 | 3·55 | 0·03 | 0·032 | 0·0145 | 0·27 |
| S3 | 0·044 | 0·60 | 0·58 | 0·95 | 1·23 | 1·65 | 0·037 | 0·023 | 0·0142 | 0·34 |
| LCS | 0·03 | – | – | 0·13 | – | – | – | 0·03 | 0·005 | 0·01 |

The $d\rho/dT$ as a function of temperature during heating of one HSLA steel (S1) and LCS are compared in Fig. 3. In the case of LCS, it shows a continuous rise

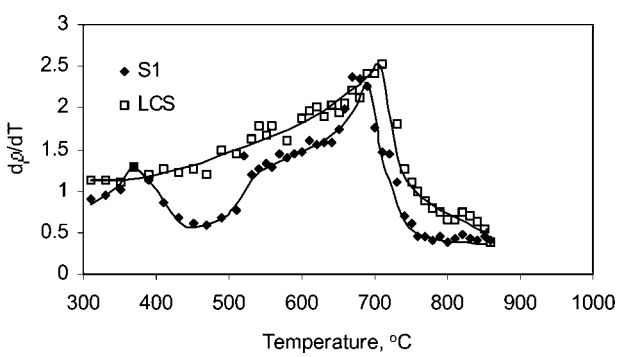


**3 Temperature coefficient of resistivity ($d\rho/dT$) as function of temperature during heating (0·33 K $s^{-1}$) of LCS and HSLA steel**

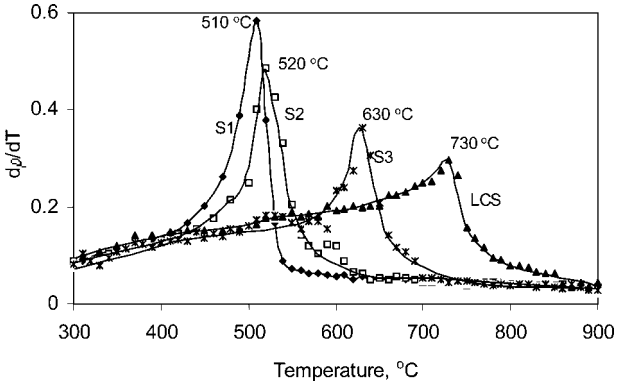


**4 Temperature coefficient of resistivity (d$\rho$/d$T$) as function of temperature during cooling (0·33 K s$^{-1}$) of LCS and HSLA steels**

revealing a peak at 720°C, whereas the steel S1 shows two peaks at 370 and at 690°C. Steels S2 and S3 also showed a similar behaviour. The peak for HSLA steel at 690°C and for LCS at 720°C coincides with the Curie temperature of the steel, whereas the peak in HSLA at 370°C can be attributed to the start of copper precipitation. The drop in Curie temperature for HSLA steel is due to the presence of alloying elements such as Mn, Ni, Si, Cu, Mo and Al.[25] During cooling, the gradient (d$\rho$/d$T$) as a function of temperature for different steels is compared in Fig. 4. In the case of each steel, it shows a peak but the temperature corresponding to the peak varies with the steel chemistry. The peak temperature can be interpreted in terms of the transformation behaviour of the austenite. When austenite transforms to bainite or martensite, a transition from paramagnetic to ferromagnetic phase occurs that causes a peak in d$\rho$/d$T$–$T$ plot and a fall in the peak temperature for all HSLA steels.

A comparison of d$\rho$/d$T$–$T$ plot during heating and cooling of HSLA and LCS is presented in Fig. 5*a–d* for S1, S2, S3 and low carbon steels respectively. The cooling curves for HSLA steels do not follow the same path as that of heating suggesting a transformation hysteresis. In contrast to this, the cooling and the heating curves practically overlap in the case of LCS. All possible transition temperatures (appearance of discontinuities) are shown in these figures. It is also clear that the peak during cooling occurs at much lower temperature than that during heating. For example, for S1 steel the peak during cooling occurs at 510°C as against at 690°C during heating. This difference may be attributed to the difference in transformation behaviour during heating and cooling. During heating, the ferromagnetic phase changes over to paramagnetic phase at the Curie temperature of the steel, whereas the reverse transition during cooling occurs in concurrent with the austenite transformation at lower temperature. The difference in the transformation behaviour causes a fall in the peak temperature during cooling.

## Dilatation measurements

Dilatation as a function of temperature during heating and cooling at a rate of 0·33 K s$^{-1}$ was recorded using Gleeble 1500 thermomechanical simulator. A typical curve during heating (at a rate of 0·33 K s$^{-1}$) and cooling (at a cooling rate of 0·33 K s$^{-1}$) for S1 steel is shown in Fig. 6. It is evident that during heating the dilatation increases with temperature linearly till a limit, beyond which there is a sudden fall, and again a linear rise upon reaching a minimum. During cooling, the dilatation decreases linearly with the fall in temperature up to a point, beyond which it rises abruptly and then it falls linearly with temperature. During heating, the deviation from linearity is associated with the $\alpha$ (bcc/bct)$\rightarrow\gamma$ transformation revealing $Ac_1$ and $Ac_3$ temperature (Table 2), while that during cooling is due to transformation of $\gamma$ to low temperature phases such as bainite. Austenite transformation temperatures ($T_s$ and $T_f$) determined from the plot are shown in Table 2.

# Discussions

In the present work, both dilatation and resistivity have been measured as a function of temperature. During heating, the transformation temperatures, such as $Ac_1$ and $Ac_3$, can be determined by the conventional dilatometry, but estimation of copper precipitation is not possible owing to its insignificant effect on the dilatation characteristics. In contrast to this, the resistivity technique is very sensitive to the alloying effect in solution, thus making it possible to estimate the amount of copper precipitation during heating; however it is difficult to estimate the transformation temperatures such as $Ac_1$ and $Ac_3$. During cooling, since the transformation from $\gamma$ to $\alpha$ causes a transition from paramagnetism to ferromagnetism, it is possible to detect the austenite transformation temperatures by resistivity as well. A comparison of the austenite transformation temperatures estimated from resistivity and dilatation is shown in Table 2. They compare well thus revealing the resistivity technique to be suitable for austenite transformation study. During austenite transformation, solubility of copper decreases leading to its precipitation, which will affect the resistivity curve but it will affect the dilatation curve very little.

Effect of different alloying elements on resistivity of iron at room temperature is documented in literature,[22,23] which can be represented as follows

$$\rho_{\text{steel}} = \rho_{\text{iron}} + 340\text{C} + 146\text{N} + 135\text{Si} + 54\text{Cr} + 50\text{Mn} + 15\text{Ni} + 34\text{Mo} + 40\text{Cu} \quad (1)$$

where, alloying elements denote the amount in wt-% in solid solution, and $\rho_{\text{steel}}$ and $\rho_{\text{iron}}$ are the resistivity of iron and steel in n$\Omega$ m.

It indicates that the resistivity of steel depends on the amount of alloying element in solid solution and its factor. The resistivity of the steel increases owing to an increase in the temperature and further rise or fall may occur owing to dissolution or precipitation of alloying elements. When an alloying element dissolves in solid solution, the resistivity increases and when it precipitates

**Table 2 Transformation temperatures estimated from dilatometric and resistivity data**

| | $Ac_1$, °C | $Ac_3$, °C | $T_S$, °C | | $T_f$, °C | |
|---|---|---|---|---|---|---|
| Steels | D* | D* | D* | R† | D* | R† |
| S1 | 693 | 801 | 553 | 550 | ~385 | ~390 |
| S2 | 690 | 803 | 585 | 590 | ~390 | ~400 |

*From dilatometric data.
†From resistivity data.

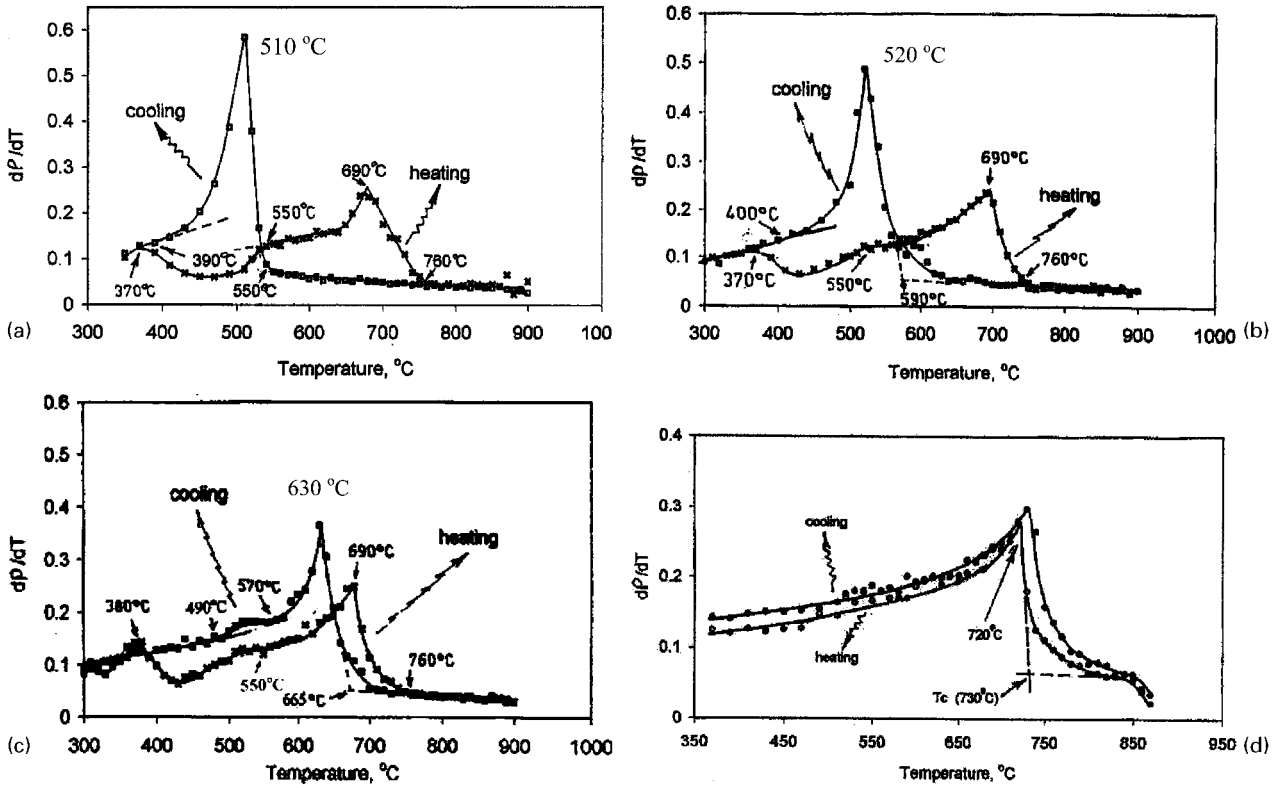


*a* S1; *b* S2; *c* S3; *d* LCS

**5 Temperature coefficient of resistivity (d$\rho$/d$T$) as function of temperature during continuous heating and cooling (0·33 K s$^{-1}$)**

out, the resistivity falls. HSLA-80 or HSLA-100 steel contains alloying elements such as Mn, Cu, Cr, Ni, Mo, Nb but either in continuously cooled or aged condition, precipitation of only copper and Nb carbide/carbonitrides has been reported.[12–16] In the steel investigated here, TEM diffraction pattern has confirmed the precipitation of copper in aged condition.[26] No evidence of the precipitates of Mn, Mo or Cr was found.[12–16,26] Thermodynamic calculation did not show the precipitation of Mn, Mo or Cr in these steels.[27] These elements will have little effect on resistivity during heating or during cooling since these will not be precipitating out. Nb generally precipitates out during hot rolling process. Further precipitation during aging of the samples quenched from 900°C or during cooling from 900°C would be very small and its effect on resistivity change will be negligible.[18] Only precipitation of copper in these steels will have a significant effect on resistivity. Therefore, the difference in the resistivity behaviour between HSLA and LCS may be attributed to the precipitation of copper from the matrix. During heating of HSLA steels, the initial dip in the d$\rho$/d$T$–$T$ curves (Fig 5*a–c*) during heating may be attributed to copper precipitation. It is to be noted that the fall was observed in all three HSLA steels in the same temperature range (about 370–550°C), whereas such behaviour was not noted in the LCS. Fujiwara *et al.*[28] have also observed a fall in the resistance in $\rho$–$T$ plot during heating of Fe–Mn–Cu alloys. They observed this phenomenon to occur in the range of 500–700°C and interpreted in terms of precipitation of some phase. In the present HSLA steels, copper is precipitating out between 370 and 550°C during heating.

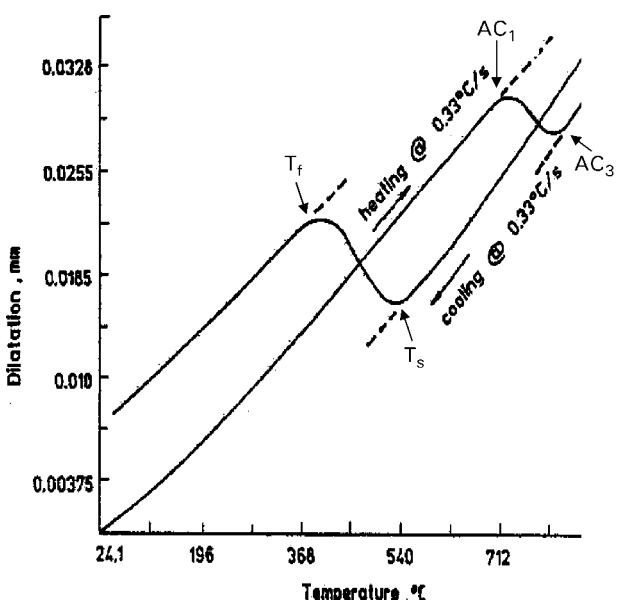


**6 Typical plot of dilatation versus temperature during heating and cooling at rate of 0·33 K s$^{-1}$ for S1 steel**

## Estimation of copper precipitation during continuous heating from resistivity data

It is known that copper precipitation occurs during aging but it is not yet known that how much copper is precipitating during heating. In the present work, an attempt was made to estimate the amount of copper precipitation during heating to various temperatures. For this, the difference in resistivity ($\Delta\rho = \rho_{HSLA} - \rho_{LCS}$) was plotted as a function of temperature, as shown in Fig. 7*a–c* for S1, S2 and S3 steels respectively. The

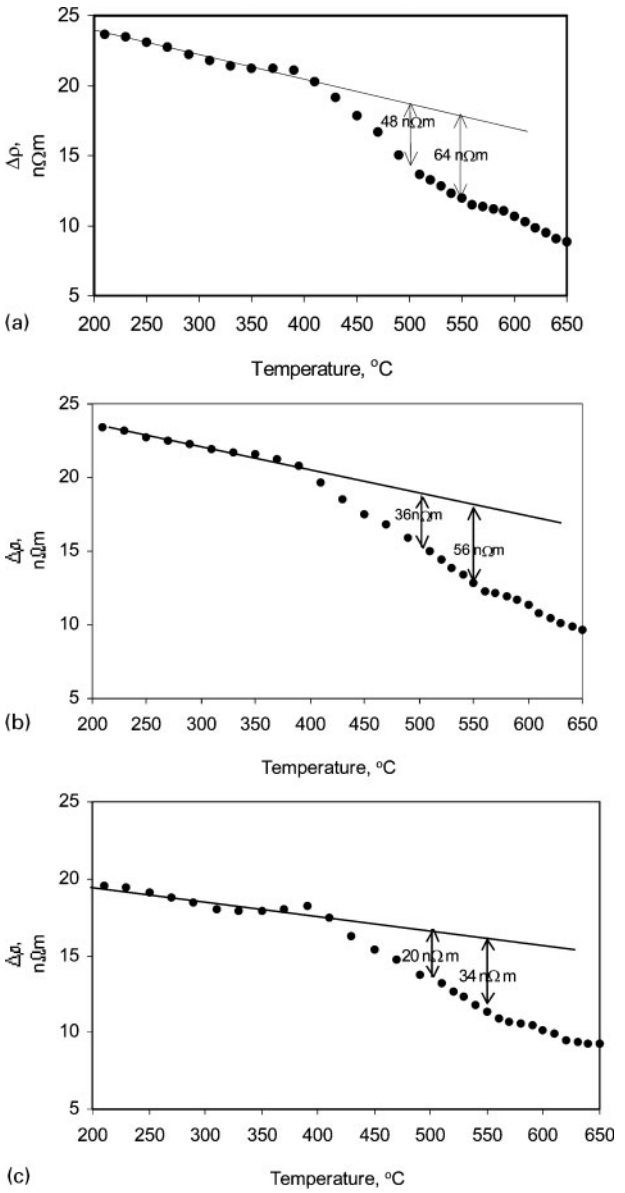


*a* S1; *b* S2; *c* S3

**7 $\Delta\rho$ (between HSLA and LCS) versus temperature to estimate amount of copper precipitation in different steels during heating; $\Delta\rho$ per wt-%Cu≡40 nΩ m[22,23]**

difference in the resistivity $\Delta\rho$ may be attributed to the precipitation of copper since LCS does not contain any copper. From equation (1), $\Delta\rho$ per wt-%Cu in pure iron=40 nΩ m.

Using this relationship, the amount of copper precipitation during heating to different temperature can be estimated. The amount of copper precipitation thus estimated for heating to 500 and 550°C is shown in Table 3, revealing that a large portion of copper is precipitating out during heating itself. The values derived from present continuous heating experiments compare well with those derived from the isothermal resistivity experiments.[26] For example, at 500 and 550°C, the amount of copper precipitation from continuous heating in S1 steel is 1·2 and 1·6 wt-% respectively, as against the 1·1 and 1·6 wt-% estimated from isothermal experiments.

## Kinetics of transformation

### *Isothermal kinetics*

Isothermal kinetics is described by Johnson–Mehl–Avrami equation[29,30] as follows

$$y = 1 - \exp[-(kt)^n] \tag{2}$$

In differential form, it becomes as

$$\frac{dy}{dt} = k(T)t^{n-1}(1-y) \tag{3}$$

### *Non-isothermal kinetics during continuous cooling*

In the case of continuous non-isothermal cooling condition, the equation may be approximated as follows[31]

$$y = 1 - \exp[-(t/\tau)^n] \tag{4}$$

where $\tau = \tau_0 \exp(-E/RT)$ and $\tau_0$ is a time constant.

In differential form, it would become as

$$\frac{dy}{dt} = \frac{1}{\tau(T)} t^{n-1}(1-y)$$

or

$$\frac{dy}{dt} = \tau_0^{-1} \exp(E/RT) t^{n-1}(1-y) \tag{5}$$

If $T_0$ is the initial temperature and the cooling rate is $B$, then

$$T = T_0 - Bt$$

then

$$dT = -B dt$$

or

$$dt = -dT/B$$

Substituting the value of $dt$ in equation (5)

$$-B\frac{dy}{dT} = \tau_0^{-1} \exp(E/RT) t^{n-1}(1-y)$$

$$\frac{-B\frac{dy}{dT}}{t^{n-1}(1-y)} / = \tau_0^{-1} \exp(E/RT) \tag{6}$$

and taking logarithm of both sides

$$\ln\left[\frac{-B\frac{dy}{dT}}{t^{n-1}(1-y)}\right] = \ln(\tau_0^{-1}) + \frac{E}{RT} \tag{7}$$

**Table 3 Amount of copper precipitation estimated from resistivity data during continuous heating**

| Steel | Total Cu in steel, wt-% | Cu ppn. during heating to 500°C, wt-% | Cu ppn. during heating to 500°C (Isothermal expt.),[26] wt-% | Cu ppn. during heating to 550°C, wt-% | Cu ppn. during heating to 550°C (Isothermal expt.),[26] wt-% |
|---|---|---|---|---|---|
| S1 | 1·98 | 1·20 | 1·14 | 1·60 | 1·62 |
| S2 | 1·58 | 0·85 | 0·77 | 1·40 | 1·38 |
| S3 | 1·23 | 0·50 | 0·62 | 0·85 | 0·81 |

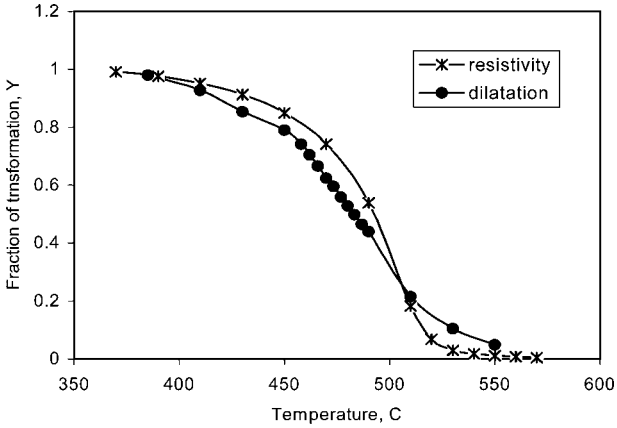


**8 Fraction of transformation *y* as function of temperature during continuous cooling measured by dilatation and resistivity technique**

Activation energy $E$ can be determined from the slope of the plot of $\ln\{(-B\mathrm{d}y/\mathrm{d}T)/[t^{n-1}(1-y)]\}$ versus $1/T$.

From dilatation as well as resistivity data obtained during continuous cooling (0·33 K $s^{-1}$) for one steel (S1), the fraction of transformation $y$ was calculated as a function of temperature, which is shown in Fig. 8. For evaluating the kinetics of transformation, the value of $n$ has been assumed to be 2. The value of $n$ during austenite transformation in similar steel has been reported[31] to be in the range of 1·8 to 2·3. The average value is taken in the present work.

$\ln\{(-B\mathrm{d}y/\mathrm{d}T)/[(1-y)t]\}$ was plotted as a function of $1/T$ using both dilatation as well as resistivity data, which reveals straight line behaviour (Fig. 9). The activation energy was derived from the slope. In the case of dilatation, it was found to be 62 kJ $mol^{-1}$. The transformation at this temperature (~550°C) is expected to result in upper bainite. Classically, the process controlling the rate of formation of upper bainite is diffusion of carbon in austenite. The activation energy of diffusion of carbon in austenite is 135 kJ $mol^{-1}$ (Ref. 32). The activation energy determined above is nearly half of that for the diffusion of carbon in austenite but can be compared well with the diffusion of carbon in ferrite (80·3 kJ $mol^{-1}$).[32] Wilson[33] also obtained an activation energy value of 79 kJ $mol^{-1}$ during isothermal transformation of upper bainite and assumed that the diffusion rate is enhanced by some

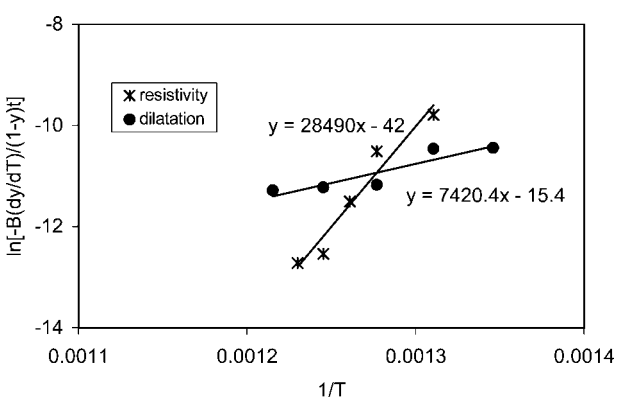


**9 Plot of $\ln\{(-B\mathrm{d}y/\mathrm{d}T)/[(1-y)t]\}$ versus $1/T$ for HSLA steel for evaluating kinetics of phase transformation during continuous cooling**

process. However, Radcliffe and Rollason[34] obtained a much lower activation energy (31·4 kJ $mol^{-1}$) for the formation of lower bainite, which can be compared with that of diffusion of carbon in ferrite.

From the resistivity data, activation energy was found to be much higher, i.e. 237 kJ $mol^{-1}$, which may correspond to the diffusion of Cu in iron (284 kJ $mol^{-1}$),[35] and is possibly associated with copper precipitation during austenite transformation. Owing to the drop in the solubility of copper during continuous cooling, it will precipitate out during austenite transformation. Interphase precipitation of Cu during continuous cooling of similar Cu bearing HSLA steel has been observed by Thompson *et al.* by TEM,[12] and the present results of kinetics using resistivity data are consistent with the observation.

## Conclusion

Resistivity technique has been applied to evaluate the austenite transformation temperatures and precipitation study in HSLA steels. A method has been demonstrated to estimate the amount of copper precipitation during continuous heating process for three copper bearing HSLA steels. Non-isothermal kinetic analysis of dilatation data during continuous cooling yields an activation energy of 62 kJ $mol^{-1}$, which is close to that of the diffusion for carbon in bainite. Resistivity data during continuous cooling reveal an activation energy of 237 kJ $mol^{-1}$, which may correspond to the diffusion of Cu in iron (284 kJ $mol^{-1}$), associated with copper precipitation during austenite transformation.

## Acknowledgement

Financial support of the Naval Research Laboratory (NRL), Washington DC, USA under grant no. N00014-95-1-0015 to carry out this work is gratefully acknowledged. One of the authors (A. N. Bhagat) also records his appreciation to Tata Steel Ltd for permission to carry out this work and publish this paper.

## References

1. E. J. Czyryca: Proc. Conf. on 'Advances in low carbon high strength ferrous alloys', (ed. O. N. Mohanty *et al.*), Vol. 84–85, 491; 1993, Switzerland, Trans. Tech. Pub.
2. M. Mujahid, A. K. Lis, C. I. Gracia and A. J. DeArdo: Proc. Conf. on 'Advances in low carbon high strength ferrous alloys', (ed. O. N. Mohanty *et al.*), Vol. 84–85, 209; 1993, Switzerland, Trans. Tech. Pub.
3. E. Hornbogen: *Trans. ASM*, 1964, **57**, 120.
4. S. R. Goodman, S. S. Brenner and J. R. Low: *Metall. Trans.*, 1973, **4**, 2371.
5. K. C. Russel and L. M. Brown: *Acta Metall.*, 1970, **20**, 969.
6. A. Deschamps, M. Militzer and W. J. Poole: *ISIJ Int.*, 2001, **41**,196.
7. K. Osamura, H. Okuda, M. Takashima, K. Asano and M. Furusaka: *JIM.*, 1993, **34**, 305.
8. E. Hornbogen and R. C. Glenn: *Trans Met. Soc. AIME*, 1960, **218**, 1064.
9. M. T. Miglin, J. P. Hirth, A. R. Rosenfield and W. A. T. Clark: *Metall. Trans. A*, 1986, **17A**, 791.
10. T. N. Lâe, A. Barbu and F. Maury: *Scr. Metall. Mater.*, 1992, **26**, 771.
11. C. S. Pande, M. A. Imam, C. L. Vold, E. Dantsker and B. B. Rath: Proc. Conf. on 'Advances in low carbon high strength ferrous alloys', (ed. O. N. Mohanty *et al.*), Vol. 84–85, 145; 1993, Switzerland, Trans. Tech. Pub.
12. S. W. Thompson and G. Krauss: *Metall. Trans. A*, 1996, **27A**, 1573.

13. D. P. Dunne, S. S. Banadkouki Ghasemi and D. Yu: *ISIJ Int.*, 1996, **36**, 324.
14. S. S. Banadkouki Ghasemi, D. Yu and D. P. Dunne: *ISIJ Int.*, 1996, **36**, 61.
15. R. Varughese and P. R. Howell: *Mater. Charact.*, 1993, **30**, 261.
16. S. W. Thompson: Proc. 40th Conf. on 'Mechanical working and steel processing', Warrendale, PA, USA, October 1998, Iron and Steel Society, 663.
17. D. T. Peter and C. R. Cupp: *Trans. AIME*, 1966, **236**, 1420.
18. R. Simoneau, G. Begin and A. H. Marquis: *Met. Sci.*, 1978, **12**, 381.
19. M. Ahmad, M. Farooque, F. H. Hasmi, S. W. Hussain and A. Q. Khan: 'Maraging steels, recent development and applications', (ed. R. K. Wilson), 269; 1988, Warrendale, PA, TMS-AIME.
20. O. N. Mohanty: *Mater. Sci. Eng. B*, 1995, **B22**, 267.
21. A. N. Bhagat: *Mater. Sci. Technol.*, 2003, **19**, 343.
22. A. L. Norbury: *JISI*, 1920, **101**, 627.
23. F. T. Sisco: 'The alloy of iron and carbon, alloy of iron reserach', 1st edn, 589; 1937, New York, McGraw Hill.
24. V. K. Bungardt and W. Spyra: *Arechiv für das Eisenhuttenwesen*, April 1965, 257.
25. O. Kubaschewski: 'Iron-binary phase diagram', 24, 32, 37, 75; 1982, Berlin, Heidelberg, Springer-Verlag.
26. A. N. Bhagat: 'Study of the phase transformation characteristics in some copper bearing HSLA steels', PhD thesis, Indian Institute of Technology (IIT) Kharagpur, India, 2002.
27. S. K. Mishra, S. Ranganathan, S. K. Das and S. Das: *Scr. Mater.*, 1998, **39**, 253.
28. S. Fujiwara, T. Shiraga and I. Tamura: *Trans. JIM*, 1976, **17**, 294.
29. M. Avrami: *J. Chem. Phys.*, 1941, **9**, 177.
30. W. A. Johnson and R. F. Mehl: *Trans. AIME*, 1939, **135**, 416.
31. M. Venkatraman, O. N. Mohanty and R. N. Ghosh: *Scand. J. Metall.*, 2001, **30**, 8.
32. A. K. Jena and M. C. Chatuvedi: 'The phase transformations in materials', 103; 1992, New Jersey, Prentice Hall.
33. E. A. Wilson: 'Worked examples in the kinetics and thermodynamics of phase transformation', 50; 1976, London, The Institution of Metallurgists.
34. S. V. Radcliffe and E. C. Rollason: *JISI*, 1959, **191**, 56.
35. E. A. Braades and G. B. Brook: 'Smithells metal reference book', 7th edn, 13–19; 1992, Oxford, Educational and Professional Publishing Ltd.